INTERNATIONAL JOURNAL OF INTEGRATED ENGINEERING
ISSN: 2229-838X e-ISSN: 2600-7916

IJIE

Vol. 16 No. 1 (2024) 143-160
https://publisher.uthm.edu.my/ojs/index.php/ijie

TSDT vs CPT and FSDT for Free Vibration Analysis of Functionally Graded Incompressible Plates

A. Naderi[1]*, E. Mohseni[2], M. Mahmoudi Saleh Abaad[1]

[1] *Department of Mechanical Engineering, Higher Education Complex of Bam, Bam, 7661314477, IRAN*
[2] *Department of Mechanical Engineering, Shahid Bahonar University of Kerman, Kerman, 76169133, IRAN*

*Corresponding Author: a.naderi@bam.ac.ir
DOI: https://doi.org/10.30880/ijie.2024.16.01.012

Article Info

Received: 18 November 2023
Accepted: 15 January 2024
Available online: 28 April 2024

Keywords

Third-order shear deformation plate theory, functionally graded incompressible materials, transverse vibration, hydrostatic pressure, bending moments

Abstract

This article studies vibrational behavior of incompressible functionally graded plates through utilizing classical, first-order shear, and third-order shear deformation plate theories. Plate material properties are presumed to differ continuously in the thickness direction concurring to a power law function. The motion and continuity equations are produced using three different plate theories, and then they are analytically solved for rectangular plates with simple supports utilizing Navier's method. The results are verified by obtaining the plate natural frequency for the power law index value equals zero and comparing them to those reported in previous works. It is shown that transverse vibrational analysis of the classical and first-order shear deformation plate theories for incompressible plates are not as precise as the compressible ones. It is shown that this issue is due to the fact that according to those theories, unlike the higher order theories, the hydrostatic pressure cannot participate in carrying the bending loads. Consequently, the equivalent flexural stiffness and as a result flexural frequencies decrease. So, to analyze the vibrational behavior of functionally graded incompressible plates, whether the plate is either thin or thick, higher order theories should be adopted. Also, it is demonstrated that TSDT is the simplest shear deformation plate theory for which the hydrostatic pressure can contribute to withstandig the bending moments. So, it can be a practical theory for free vibration analysis of functionally graded incompressible plates. Finally, this theory has been taken into consideration to analyze the vibrational behavior of rectangular plates made of functionally graded incompressible materials Also detailed parametric studies have been carried out.

1. Introduction

Polymers, elastomers, rubbers and living tissues are characterized as incompressible materials whose deformations are isochoric or volume preserving. On the other hand, functionally graded materials have some features including that they are continuously inhomogeneous composites constituted from two or more materials. The material properties of functionally graded materials can generally be constructed technologically in order to fulfill several performance requirements in diverse parts of a structure or machine. However, constitutes of a functionally graded material can be from incompressible materials. Functionally graded incompressible materials can generally be exploited in different structural and mechanical elements such as plates.

Unlike the incompressible ones, there are too many studies on the mechanical behavior of plates made from compressible FG materials. For example, upon utilizing Reddy's higher order shear deformation plate theory, Pham et al. [1] established an analytical approach to investigate bucking and post-buckling behavior of functionally graded porous plates resting on elastic foundation. Nwoji et al. [2] utilized the Ritz method to solve bending problem of rectangular Kirchhoff plates subjected to distribution of a transverse hydrostatic load over the domain of the entire plate. Naderi and Saidi [3] presented an analytical solution for buckling of functionally graded sector plates resting on an elastic foundation. Demirhan and Taskin [4] investigated free vibration and bending characteristics of porous functionally graded plates based on a refined four variable plate theory. Singh and Harsha [5] investigated buckling problem of functionally graded plates through exploiting a non-polynomial based higher order shear deformation plate theory. Abdollahi et al. [6] investigated buckling analysis of thick functionally graded piezoelectric rectangular plates based on the higher order shear and normal deformable plate theory. Rouzegar and Abad [7] represented an analytical solution for free vibration analysis of a functionally graded plate integrated with piezoelectric layers considering four-variable refined plate theory. Mojahedin et al. [8] presented the buckling analysis of radially loaded solid circular plate made of functionally graded porous materials. Ebrahimi and Habibi [9] studied bending and vibration characteristics of saturated porous functionally graded rectangular plates by using the third-order shear deformation plate theory. Chiker et al. [10] studied free vibration problem of hybrid laminated plates including multilayer functionally graded carbon nanotube-reinforced composite plies. Rezaei et al. [11] developed free vibration analysis of functionally graded porous rectangular plates . Cho [12] introduced hierarchic models for vibration analysis of ceramic–metal functional gradient plates. Hashemi et al [13] presented an exact solution for vibration problem of functionally graded annular plates with elastic edges supports resting on Winkler foundation. Ghatage and Sudhagar [14] studied free vibrational behavior of bi-directional functionally graded composite panel with and without porosities using 3D finite element approximations. Ghatage et al. [15] presented an exhaustive review on modelling and analysis of multi-directional graded (beam/plate/shell) structures. Chaudhary et al. [16] examined flexural behavior of functionally graded composite panels with single and multiple rectangular perforations under complex loading conditions. Ghatage and Sudhagar [17] studied free vibration of bi-directional axially graded cylindrical shell panels using 3D graded finite element approximation under a temperature field. Kar et al. [18] examined numerically post-buckling behavior of functionally graded shell panels subjected to uniform and non-uniform thermal environment considering a nonlinear finite element method. Joshi et. al [19] illustrated various micromechanical modelling schemes that are applied to obtain the effective mechanical properties of functionally graded materials such as plates, shells, panels, and beams. Ghatage et. al [20] examined natural frequencies of biaxial functionally graded panels. Also, Gaspar et. al [21] represented the static and vibrational behaviors of functionally graded plane structures, such as plane truss and frame-type structures.

Generally, incompressible materials can withstand only isochoric deformations, i.e. they can only bear pure distortional deformations. Because of this constraint, the constitutive relations involve a hydrostatic pressure which cannot be obtained from the strain components, but it is obtainable from a solution of the governing equations together with the specified initial and boundary conditions. In this regard, Herrmann [22] presented the linear elasticity equations which can be applied to both compressible and incompressible materials. These equations involved four unknowns including three components of displacement and one for the hydrostatic pressure.

Some researchers have studied the mechanical behavior of homogeneous isotropic incompressible plates. For example, Batra and Aimmanee [23] analyzed vibration of a homogeneous rectangular plate made of an incompressible linear elastic material using a mixed higher-order shear and normal deformable plate theory considering Poisson's ratio value equal to 0.49 and employing the finite element method. Aimmanee and Batra [24] established an analytical solution for free vibration of a simply supported rectangular plate made of a homogeneous incompressible linear elastic isotropic material. Yuan and Batra [25] developed free vibrations of homogeneous incompressible rectangular plates subjected to diverse boundary conditions using the third-order shear and normal deformable theory and the finite element method. However, there are a few works on the mechanical behavior of inhomogeneous incompressible plates. In this regarding, Batra [26] derived the equations of motion for a plate composed of a linear elastic functionally graded incompressible material exploiting the higher-order shear and normal deformable plate theory. Nevertheless, there was no mention of a solution for those equations in that work. Mohammadi et al. [27] developed the static, dynamic and stability responses of functionally graded incompressible linear elastic plates using higher order shear and normal deformable plate theory. They solved the governing equations analytically using the Navier's method.

Generally, compared to 3D theories (such as 3D elasticity theory and higher-order shear and normal deformable plate theory), solution procedure of the plate problems utilizing the plate theories (such as classical, first order shear deformation and third-order shear deformation plate theories) is less complicated. To the best knowledge of the author's, vibration analysis of functionally graded incompressible plates has been done only based on the higher-order shear and normal deformable plate theory but the other plate theories such as classical, first order shear deformation and third order shear deformation theories have not been examined yet.

Int. Journal of Integrated Engineering Vol. 16 No. 1 (2024) p. 143-160

This article studies vibrational behavior of incompressible functionally graded plates utilizing classical, first-order shear deformation, and third-order shear deformation plate theories. FG plate material properties are assumed to differ through the thickness direction of the plate according to the power law function. Governing equation of motion together with the incompressibility equation are solved exactly for rectangular plates with simple supports. The results are compared with those reported in previous works. It is shown that for the flexural vibrational analysis, the classical and first-order shear deformation plate theories for incompressible plates are not as accurate as for the compressible ones. It is shown that this issue refers to the fact that these theories generally consider the hydrostatic pressure as a constant along the plate thickness direction and consequently no bending moment is undergone due to the hydrostatic pressure. However, it is shown that considering the third-order shear deformation plate theory, the hydrostatic pressure because of its variable distribution along the plate thickness direction, can participate in sustaining the bending loads. Consequently, although in comparison with TSDT it seems that CPT and FSDT should cause to larger bending natural frequencies, it is observed that TSDT presents larger ones. It is concluded that generally, to obtain frequencies from the free vibration analysis of incompressible functionally graded plates to be acceptable, whether the plate is either thin or thick, higher-order plate theories should be developed. Finally, natural frequencies of the incompressible FG plate are attained using the third-order shear deformation plate theory for several thickness ratio values, aspect ratio values, power law index values and mode number values. In addition, the plate mode shapes are plotted and the power law effects on the mode shape plots are discussed in detail.

2. Kinematics

Consider a rectangular plate with length *a*, width *b* and uniform thickness *h* composed of an incompressible linear elastic functionally graded material as depicted in Fig. 1. Also, consider x_1 and x_2 to be in-plane and x_3 to be out of plane (thickness) coordinates of the plate. The vibrational behavior of such plate is investigated here according to three following plate theories.

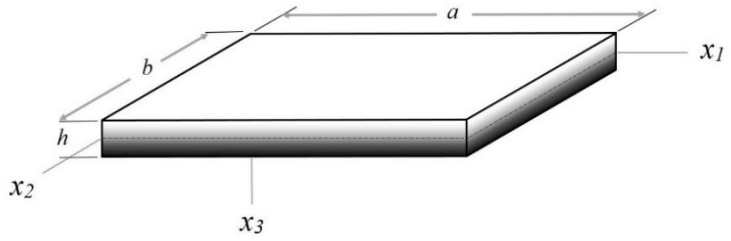

Fig. 1 *The geometry and coordinate system of the incompressible functionally graded plate*

2.1 CPT

The classical plate theory (CPT) is least complicated plate theory not considering the effects of shear and normal deformations in the thickness direction [28, 29]. Although this theory is a good choice for different mechanical analysis of thin plates made from common compressible materials, its accuracy has not been investigated yet for thin plates made from incompressible materials. The plate displacement field and also the internal hydrostatic pressure *p* within this theory are assumed as follows

$$u_1(x_1,x_2,x_3,t) = u(x_1,x_2,t) - x_3\frac{\partial w}{\partial x_1} \tag{1-1}$$

$$u_2(x_1,x_2,x_3,t) = v(x_1,x_2,t) - x_3\frac{\partial w}{\partial x_2} \tag{1-2}$$

$$u_3(x_1,x_2,x_3,t) = w(x_1,x_2,t) \tag{1-3}$$

$$p(x_1,x_2,x_3,t) = p_0(x_1,x_2,t) \tag{1-4}$$

where *u*, *v* and *w*, are the mid-plane components of the displacement field. As can be seen from equations (1), the hydrostatic pressure *p* has been posed to be constant through the plate thickness direction. Using equations (1), the strain-displacement relations based on CPT formulation can be written as follows

$$\begin{Bmatrix} \varepsilon_{11} \\ \varepsilon_{22} \\ \varepsilon_{33} \\ \gamma_{12} \\ \gamma_{13} \\ \gamma_{23} \end{Bmatrix} = \begin{Bmatrix} u_{,1} - x_3 w_{,11} \\ v_{,2} - x_3 w_{,22} \\ 0 \\ u_{,2} + v_{,1} - 2x_3 w_{1,2} \\ 0 \\ 0 \end{Bmatrix} \tag{2}$$

in which the subscript "," represents partial differentiation respecting to x_1 and x_2.

2.2 FSDT

Unlike CPT, the first-order shear deformation plate theory (FSDT) takes the shear deformations along the thickness direction into account [30-32]. This theory, however, presents a good accuracy for different structural analyses of moderately thick plates made from compressible materials. Conversely, its accuracy for incompressible moderately thick plates has not been examined yet. According to FSDT, the displacement field and the internal hydrostatic pressure p for an incompressible plate are written in the following form

$$u_1(x_1, x_2, x_3, t) = u(x_1, x_2, t) + x_3\theta_1(x_1, x_2, t) \tag{3-1}$$
$$u_2(x_1, x_2, x_3, t) = v(x_1, x_2, t) + x_3\theta_2(x_1, x_2, t) \tag{3-2}$$
$$u_3(x_1, x_2, x_3, t) = w(x_1, x_2, t) \tag{3-3}$$
$$p(x_1, x_2, x_3, t) = p_0(x_1, x_2, t) \tag{3-4}$$

where θ_1 and θ_2 are the rotations of a transverse normal line about x_1 and x_2 axes, respectively, are defined as

$$\theta_1 = \left(\frac{\partial u_1}{\partial x_3}\right), \ \theta_2 = \left(\frac{\partial u_2}{\partial x_3}\right) \tag{4}$$

It is noticeable that according to the relation (3-4), the hydrostatic pressure p is considered to be independent of the out of plane coordinate, x_3. Also, the strain-displacement relations for FSDT formulation can be addressed in the following form

$$\begin{Bmatrix} \varepsilon_{11} \\ \varepsilon_{22} \\ \varepsilon_{33} \\ \gamma_{12} \\ \gamma_{13} \\ \gamma_{23} \end{Bmatrix} = \begin{Bmatrix} u_{,1} + x_3\theta_1 \\ v_{,2} + x_3\theta_2 \\ 0 \\ u_{,2} + v_{,1} + x_3\left(\theta_{1,2} + \theta_{2,1}\right) \\ \theta_1 + w_{,1} \\ \theta_2 + w_{,2} \end{Bmatrix} \tag{5}$$

2.3 TSDT

Third order shear deformation plate theory (TSDT) accounts for through the thickness shear deformations [33] but in a more accurate manner than FSDT. However, to the best knowledge of the author's, this theory has not been dealt with yet for vibrational analysis of plates made from incompressible materials. The displacement components and also the hydrostatic pressure field based on this theory are written in the following form

$$u_1(x_1, x_2, x_3, t) = u(x_1, x_2, t) + x_3\theta_1(x_1, x_2, t) + x_3^2\varphi_1(x_1, x_2, t) + x_3^3\psi_1(x_1, x_2, t) \tag{6-1}$$
$$u_2(x_1, x_2, x_3, t) = v(x_1, x_2, t) + x_3\theta_y(x_1, x_2, t) + x_3^2\varphi_y(x_1, x_2, t) + x_3^3\psi_y(x_1, x_2, t) \tag{6-2}$$
$$u_3(x_1, x_2, x_3, t) = w(x_1, x_2, t) + x_3\theta_z(x_1, x_2, t) + x_3^2\varphi_z(x_1, x_2, t) \tag{6-3}$$
$$p(x_1, x_2, x_3, t) = p_0(x_1, x_2, t) + x_3 p_1(x_1, x_2, t) + x_3^2 p_2(x_1, x_2, t) \tag{6-4}$$

where

$$\theta_1 = \left(\frac{\partial u_1}{\partial x_3}\right)_{x_3=0}, \ \theta_2 = \left(\frac{\partial u_2}{\partial x_3}\right)_{x_3=0}, \ \theta_3 = \left(\frac{\partial u_3}{\partial x_3}\right)_{x_3=0}$$
$$\varphi_1 = \frac{1}{2}\left(\frac{\partial^2 u_1}{\partial x_3^2}\right)_{x_3=0}, \ \varphi_2 = \frac{1}{2}\left(\frac{\partial^2 u_2}{\partial x_3^2}\right)_{x_3=0}, \ \varphi_3 = \frac{1}{2}\left(\frac{\partial^2 u_3}{\partial x_3^2}\right)_{x_3=0} \tag{7}$$

Int. Journal of Integrated Engineering Vol. 16 No. 1 (2024) p. 143-160

$$\psi_1 = \frac{1}{6}\left(\frac{\partial^3 u_1}{\partial x_3^2}\right)_{x_3=0}, \quad \psi_2 = \frac{1}{6}\left(\frac{\partial^3 u_2}{\partial x_3^2}\right)_{x_3=0}$$

Comparison of the equation (6-4) with the equations (1-4) and (3-4) shows that unlike CPT and FSDT, TSDT considers the hydrostatic pressure p to be varied through the plate thickness direction. Utilizing the equations (6-1) to (6-4), it is easy to show that the strain-displacement relations for TSDT formulation can be written in the following form

$$\begin{Bmatrix} \varepsilon_{11} \\ \varepsilon_{22} \\ \varepsilon_{33} \\ \gamma_{12} \\ \gamma_{13} \\ \gamma_{23} \end{Bmatrix} = \begin{Bmatrix} u_{,1} + x_3\theta_{1,1} + x_3^2\varphi_{1,1} + z^3\psi_{1,1} \\ v_{,2} + x_3\theta_{2,2} + z^2\varphi_{2,2} + z^3\psi_{2,2} \\ \theta_3 + 2x_3\varphi_3 \\ u_{1,2} + u_{2,1} + x_3(\theta_{1,2} + \theta_{2,1}) + x_3^2(\varphi_{1,2} + \varphi_{2,1}) + x_3^3(\psi_{1,2} + \psi_{2,1}) \\ \theta_1 + 2x_3\varphi_1 + 3x_3^2\psi_1 + w_{,1} + x_3\theta_{3,1} + x_3^2\psi_{3,1} \\ \theta_2 + 2x_3\varphi_2 + 3x_3^2\psi_2 + w_{,2} + x_3\theta_{3,2} + x_3^2\psi_{3,2} \end{Bmatrix} \tag{8}$$

3. Constitutive Relations

The plate is presumed to be constituted of two incompressible materials with a continuous variation of the volume fraction of its constituents through the plate thickness direction. In the following, the constitutive equations and the material properties are presented for such a plate.

3.1 Constitutive Relations for Incompressible Materials

The stress components for an incompressible material considering the incompressibility condition are represented as follows [26]

$$\sigma_{ij} = -p\delta_{ij} + \hat{\sigma}_{ij} \tag{9}$$

where p is the generated hydrostatic pressure in the body, δ_{ij} is Kroncker delta function and $\hat{\sigma}_{ij}$ is Cauchy stress related to the infinitesimal strain components for a linear isotropic material as follows

$$\hat{\sigma}_{ij} = 2\mu\varepsilon_{ij} + \lambda\varepsilon_{kk}\delta_{ij} \tag{10}$$

where, λ and μ are Lamè constants. Replacing equation (10) into equation (9) leads to

$$\sigma_{ij} = -p\delta_{ij} + 2\mu\varepsilon_{ij} + \lambda\varepsilon_{kk}\delta_{ij} \tag{11}$$

For incompressible materials, the relative volume variation ε_{kk} equals zero [34]. Therefore, the stress-strain relation for an incompressible isotropic linear elastic material in equation (11) can be rewritten in the following form [34]

$$\sigma_{ij} = -p\delta_{ij} + 2\mu\varepsilon_{ij} \tag{12}$$

3.2 Material Properties Distribution

It is presumed here that the plate material properties differ continuously from top to bottom surfaces according to the following power law function [35]

$$\Gamma(x_3) = (\Gamma_1 - \Gamma_2)\left(\frac{1}{2} + \frac{x_3}{h}\right)^N + \Gamma_2 \tag{13}$$

where Γ refers to a typical material property value, such as Young's modulus E, density ρ or Lame constants λ and μ. Also, indices 1 and 2 refer to the bottom and top surfaces material, respectively. Moreover, x_3 is the plate thickness coordinate and N is the power-law index indicating volume fraction of the components.

4. Governing Equations

The equations of motion of the plate can be determined using Hamilton's principle, stating that [36]

$$\int_0^T (\delta U + \delta V - \delta K)dT = 0 \tag{14}$$

where δ represents the variational symbol, δU and δK express the virtual strain energy and the virtual kinetic energy of the plate, respectively, defined as

$$\delta U = \int_{\Omega}\int_{-\frac{h}{2}}^{\frac{h}{2}} (\sigma_{11}\delta\varepsilon_{11} + \sigma_{22}\delta\varepsilon_{22} + \sigma_{33}\delta\varepsilon_{33} + \sigma_{12}\delta\gamma_{12} + \sigma_{13}\delta\gamma_{13} + \sigma_{23}\delta\gamma_{23})dx_3 d\Omega \tag{15-1}$$

$$\delta K = \int_{\Omega}\int_{-\frac{h}{2}}^{\frac{h}{2}} \rho(\frac{\partial u_1}{\partial t}\frac{\partial \delta u_1}{\partial t} + \frac{\partial u_2}{\partial t}\frac{\partial \delta u_2}{\partial t} + \frac{\partial u_3}{\partial t}\frac{\partial \delta u_3}{\partial t})dx_3 d\Omega \tag{15-2}$$

in which Ω indicates the area of the mid-plane.

Also, δV is the virtual potential energy of external loads. Since it is assumed here that no external force is applied to the plate, one can obtain $\delta V=0$. It is noticeable that due to the incompressibility effects, the continuity equation should be also satisfied for the plate as follows

$$\varepsilon_{kk} = 0 \Rightarrow \frac{\partial u_1}{\partial x_1} + \frac{\partial u_2}{\partial x_2} + \frac{\partial u_3}{\partial x_3} = 0 \tag{16}$$

In the following, the equations of motion together with the incompressibility equation are derived applying different plate theories.

4.1 CPT

Through using the relations (1), (2), (15) and (16), the equations of motion based on the classical plate theory (CPT) can be written as the follows

$$-I_0\ddot{u} + I_1\frac{\partial \ddot{w}}{\partial x_1} + \frac{\partial M_1^0}{\partial x_1} + \frac{\partial M_{12}^0}{\partial x_2} = 0 \tag{17-1}$$

$$-I_0\ddot{v} + I_1\frac{\partial \ddot{w}}{\partial x_2} + \frac{\partial M_{12}^0}{\partial x_1} + \frac{\partial M_2^0}{\partial x_2} = 0 \tag{17-2}$$

$$-I_0\ddot{w} - I_1(\frac{\partial \ddot{u}}{\partial x_1} + \frac{\partial \ddot{v}}{\partial x_2}) + I_2\nabla^2\ddot{w} + \frac{\partial^2 M_1^1}{\partial x_1^2} + 2\frac{\partial^2 M_{12}^1}{\partial x_1 x_2} + \frac{\partial^2 M_2^1}{\partial x_2^2} = 0 \tag{17-3}$$

in which, the stress resultants are defined as

$$M_{\alpha\beta}^j = \int_{-\frac{h}{2}}^{\frac{h}{2}} \sigma_{11} x_3^j dx_3, \quad j = 0,1, \quad \alpha,\beta = 1,2 \tag{18}$$

and also, the moment inertias are defined as the following form

$$I_j = \int_{-\frac{h}{2}}^{\frac{h}{2}} \rho x_3^j dx_3, \quad j = 0,1 \tag{19}$$

Substituting equation (18) together with equations (12), (2) and (4-1) into relations (17), one can determine the equations of motion in terms of the displacement components. It should be noted that since the hydrostatic pressure p is considered to be independent of the plate thickness coordinate, it plays no role in the bending moments obtained from the relation (18) and consequently in the transverse motion equation (17-3). Therefore, based on CPT, the hydrostatic pressure p has no effect on bearing the bending loadings.

Obviously, the continuity condition in equation (16) should be also satisfied together with the equations of motion. For this purpose, one can multiply both sides of the equation (16) by a virtual function $\delta\mu=\delta\mu_0(x_1,x_2,t)$ and integrate it over the plate domain, which leads to the following relation

$$\frac{\partial u}{\partial x_1} + \frac{\partial v}{\partial x_2} = 0 \tag{20}$$

4.2 FSDT

Performing the same procedure that has been done for CPT in the subsection (4.1), the equations of motion applying the first-order shear deformation plate theory (FSDT) are obtainable as bellows

$$-I_0\ddot{u} - I_1\ddot{\varphi}_1 + \frac{\partial M_1^0}{\partial x_1} + \frac{\partial M_{12}^0}{\partial x_2} = 0 \tag{21-1}$$

Int. Journal of Integrated Engineering Vol. 16 No. 1 (2024) p. 143-160

$$-I_0\ddot{v}-I_1\ddot{\varphi}_2+\frac{\partial M_{12}^0}{\partial x_1}+\frac{\partial M_2^0}{\partial x_2}=0 \tag{21-2}$$

$$-I_0\ddot{w}+\frac{\partial T_1^0}{\partial x_1}+\frac{\partial T_2^0}{\partial x_2}=0 \tag{21-3}$$

$$-I_1\ddot{u}-I_2\ddot{\varphi}_1+\frac{\partial M_1^1}{\partial x_1}+\frac{\partial M_{12}^1}{\partial x_2}-T_1^0=0 \tag{21-4}$$

$$-I_1\ddot{v}-I_2\ddot{\varphi}_2+\frac{\partial M_{12}^1}{\partial x_1}+\frac{\partial M_2^1}{\partial x_2}-T_2^0=0 \tag{21-5}$$

where

$$M_{\alpha\beta}^j=\int_{-\frac{h}{2}}^{\frac{h}{2}}\sigma_{\alpha\beta}x_3^j dx_3,\ \ j=0,1,\ \ \alpha,\beta=1,2 \tag{22-1}$$

$$T_\alpha^j=\int_{-\frac{h}{2}}^{\frac{h}{2}}k_s\sigma_{13}x_3^j dx_3,\ \ j=0,\ \ \alpha=1,2 \tag{22-2}$$

and

$$I_j=\int_{-\frac{h}{2}}^{\frac{h}{2}}\rho x_3^j dx_3,\ \ j=0,1,2 \tag{23}$$

where, k_s is the shear correction factor. It should be noted that FSDT, the same as CPT, does not account for the hydrostatic pressure in the transverse equations of motion (equations (21-3) to (21-5)). This issue, however, refers to the fact that similar to CPT, the hydrostatic pressure p has been considered to be independent of the thickness coordinate and consequently, it will not be appeared in the relations of the bending moments.

Also, carrying the already described procedure out, the continuity condition based on the first order shear deformation theory can be obtained in the following form

$$\frac{\partial u}{\partial x_1}+\frac{\partial v}{\partial x_2}=0 \tag{24}$$

The equation (24) should be solved together with the equations of motion presented in relations (21).

4.3 TSDT

Using Hamilton's principle in equation (14) together with equations (8), (12) and (15), the equations of motion based on the third-order shear deformation plate theory (TSDT), can be expressed as follows

$$-I_0\ddot{u}-I_1\ddot{\theta}_1-I_2\ddot{\varphi}_1-I_3\ddot{\psi}_1+\frac{\partial M_1^0}{\partial x_1}+\frac{\partial M_{12}^0}{\partial x_2}=0 \tag{25-1}$$

$$-I_0\ddot{v}-I_1\ddot{\theta}_2-I_2\ddot{\varphi}_2-I_3\ddot{\psi}_2+\frac{\partial M_2^0}{\partial x_2}+\frac{\partial M_{12}^0}{\partial x_1}=0 \tag{25-2}$$

$$-I_0\ddot{w}-I_1\ddot{\theta}_3-I_2\ddot{\varphi}_3+\frac{\partial T_1^0}{\partial x_1}+\frac{\partial T_2^0}{\partial x_2}=0 \tag{25-3}$$

$$-I_1\ddot{u}-I_2\ddot{\theta}_1-I_3\ddot{\varphi}_1-I_4\ddot{\psi}_1+\frac{\partial M_1^1}{\partial x_1}+\frac{\partial M_{12}^1}{\partial x_2}-T_1^0=0 \tag{25-4}$$

$$-I_1\ddot{v}-I_2\ddot{\theta}_2-I_3\ddot{\varphi}_2-I_4\ddot{\psi}_2+\frac{\partial M_2^1}{\partial x_2}+\frac{\partial M_{12}^1}{\partial x_1}-T_2^0=0 \tag{25-5}$$

$$-I_1\ddot{w}-I_2\ddot{\theta}_3-I_3\ddot{\varphi}_3+\frac{\partial T_1^0}{\partial x_1}+\frac{\partial T_2^0}{\partial x_2}-T_3^0=0 \tag{25-6}$$

$$-I_2\ddot{u}-I_3\ddot{\theta}_1-I_4\ddot{\varphi}_1-I_5\ddot{\psi}_1+\frac{\partial M_1^2}{\partial x_1}+\frac{\partial M_{12}^2}{\partial x_2}-2T_1^1=0 \tag{25-7}$$

$$-I_2\ddot{v}-I_3\ddot{\theta}_2-I_4\ddot{\varphi}_2-I_5\ddot{\psi}_2+\frac{\partial M_2^2}{\partial x_2}+\frac{\partial M_{12}^2}{\partial x_1}-2T_2^1=0 \tag{25-8}$$

$$-I_2\ddot{w}-I_3\ddot{\theta}_3-I_4\ddot{\varphi}_3+\frac{\partial T_1^1}{\partial x_1}+\frac{\partial T_2^1}{\partial x_2}-2M_3^1=0 \tag{25-9}$$

$$-I_3\ddot{u}-I_4\ddot{\theta}_1-I_5\ddot{\varphi}_1-I_6\ddot{\psi}_1+\frac{\partial M_1^3}{\partial x_1}+\frac{\partial M_{12}^3}{\partial x_2}-2T_1^2=0 \tag{25-10}$$

$$-I_3\ddot{v}-I_4\ddot{\theta}_2-I_5\ddot{\varphi}_2-I_6\ddot{\psi}_2+\frac{\partial M_2^3}{\partial x_2}+\frac{\partial M_{12}^3}{\partial x_1}-2T_2^2=0 \tag{25-11}$$

where, the stress resultants are defined as

$$M_{\alpha\beta}^j=\int_{-\frac{h}{2}}^{\frac{h}{2}}\sigma_{\alpha\beta}x_3^j dx_3,\ \ j=0,1,2,3,\ \ \alpha,\beta=1,2 \tag{26-1}$$

$$T_\alpha^j=\int_{-\frac{h}{2}}^{\frac{h}{2}}\sigma_{\alpha 3}x_3^j dx_3,\ \ j=0,1,2,\ \ \alpha=1,2 \tag{26-2}$$

$$T_\alpha^j=\int_{-\frac{h}{2}}^{\frac{h}{2}}\sigma_{\alpha}x_3^j dx_3,\ \ j=0,1,\ \ \alpha=3 \tag{26-3}$$

also, the moment inertias are defined as the form

$$I_j=\int_{-\frac{h}{2}}^{\frac{h}{2}}\rho x_3^j dx_3,\ \ j=0,1,...,6 \tag{27}$$

Substituting equations (23) together with equations (12), (8) and (6-4) into relations (22), one can obtain the equations of motion in terms of the displacement components and also the hydrostatic pressure parameters. It is noticeable that, according to TSDT, the hydrostatic pressure p is appeared also in the out-of-plane equations of motion because of its variable distribution in the thickness direction (see the relation (6-4)). As a result, unlike CPT and FSDT, according to TSDT, the hydrostatic pressure p contributes to bearing the bending loadings, resulting in the plate to behave stiffer.

In order to fulfil the continuity condition, similar to the previous two cases, a virtual function $\delta\mu$ is considered in accordance with the corresponding hydrostatic pressure distribution, as follows

$$\delta\mu(x_1,x_2,x_3,t)=\delta\mu_0(x_1,x_2,t)+x_3\delta\mu_1(x_1,x_2,t)+x_3^2\delta\mu_2(x_1,x_2,t) \tag{28}$$

Multiplying the continuity equation (16) by $\delta\mu$ and integrating it over the plate domain, it can lead to the following expressions for the incompressibility condition of the plate based on the third-order shear deformation plate theory.

$$(\frac{\partial u}{\partial x_1}+\frac{\partial v}{\partial x_2}+\theta_3)h+(\frac{\partial\varphi_1}{\partial x_1}+\frac{\partial\varphi_2}{\partial x_2})\frac{h^3}{12}=0 \tag{29-1}$$

$$(\frac{\partial\theta_1}{\partial x_1}+\frac{\partial\theta_2}{\partial x_2}+2\varphi_2)\frac{h^3}{12}+(\frac{\partial\psi_1}{\partial x_1}+\frac{\partial\psi_2}{\partial x_2})\frac{h^5}{80}=0 \tag{29-2}$$

$$(\frac{\partial u}{\partial x_1}+\frac{\partial v}{\partial x_2}+\theta_1)h+(\frac{\partial\varphi_1}{\partial x_1}+\frac{\partial\varphi_2}{\partial x_2})\frac{h^3}{12}=0 \tag{29-3}$$

In the following, the governing differential equations are solved analytically to find the natural frequencies.

5. Analytical Solutions

It is presumed that the incompressible functionally graded rectangular plate has simple supports along with all edges. Upon using Hamilton's principle, the boundary conditions based on CPT, FSDT and TSDT are written as described in Table 1.

Table 1 *Simply supported boundary conditions of the plate based on different plate theories*

$on\ \ x_1=0,a\Rightarrow$	$w=\theta_3=\varphi_3=0$	
	$M_{11}^j=M_{21}^j=0$	$CPT:\ j=0,1$
		$FSDT:\ j=0,1$
		$TSDT:\ j=0,1,2,3$
$on\ x_2=0,b\Rightarrow$	$w=\theta_3=\varphi_3=0$	
	$M_{22}^j=M_{12}^j=0$	$CPT:\ j=0,1$
		$FSDT:\ j=0,1$
		$TSDT:\ j=0,1,2,3$

Int. Journal of Integrated Engineering Vol. 16 No. 1 (2024) p. 143-160

According to the mentioned boundary conditions in Table 1 along with the stress-resultants obtained in terms of the displacement and the hydrostatic pressure components, one can write the solutions of the governing differential equations (motion and incompressibility) as follows

$$u(x_1,x_2,t)=e^{i\omega t}\sum_{m,n=1} U^{mn}\cos(\alpha x_1)\sin(\beta x_2) \tag{30-1}$$

$$v(x_1,x_2,t)=e^{i\omega t}\sum_{m,n=1} V^{mn}\sin(\alpha x_1)\cos(\beta x_2) \tag{30-2}$$

$$w(x_1,x_2,t)=e^{i\omega t}\sum_{m,n=1} W^{mn}\sin(\alpha x_1)\sin(\beta x_2) \tag{30-3}$$

$$\theta_1(x_1,x_2,t)=e^{i\omega t}\sum_{m,n=1} \Theta_1^{mn}\cos(\alpha x_1)\sin(\beta x_2) \tag{30-4}$$

$$\theta_2(x_1,x_2,t)=e^{i\omega t}\sum_{m,n=1} \Theta_2^{mn}\sin(\alpha x_1)\cos(\beta x_2) \tag{30-5}$$

$$\theta_3(x_1,x_2,t)=e^{i\omega t}\sum_{m,n=1} \Theta_3^{mn}\sin(\alpha x_1)\sin(\beta x_2) \tag{30-6}$$

$$\Phi_1(x_1,x_2,t)=e^{i\omega t}\sum_{m,n=1} \Phi_1^{mn}\cos(\alpha x_1)\sin(\beta x_2) \tag{30-7}$$

$$\Phi_2(x_1,x_2,t)=e^{i\omega t}\sum_{m,n=1} \Phi_2^{mn}\sin(\alpha x_1)\cos(\beta x_2) \tag{30-8}$$

$$\Phi_3(x_1,x_2,t)=e^{i\omega t}\sum_{m,n=1} \Phi_3^{mn}\sin(\alpha x_1)\sin(\beta x_2) \tag{30-9}$$

$$\psi_1(x_1,x_2,t)=e^{i\omega t}\sum_{m,n=1} \Psi_1^{mn}\cos(\alpha x_1)\sin(\beta x_2) \tag{30-10}$$

$$\psi_2(x_1,x_2,t)=e^{i\omega t}\sum_{m,n=1} \Psi_2^{mn}\sin(\alpha x_1)\cos(\beta x_2) \tag{30-11}$$

$$p_0(x_1,x_2,t)=e^{i\omega t}\sum_{m,n=1} P_0^{mn}\sin(\alpha x_1)\sin(\beta x_2) \tag{30-12}$$

$$p_1(x_1,x_2,t)=e^{i\omega t}\sum_{m,n=1} P_1^{mn}\sin(\alpha x_1)\sin(\beta x_2) \tag{30-13}$$

$$p_2(x_1,x_2,t)=e^{i\omega t}\sum_{m,n=1} P_2^{mn}\sin(\alpha x_1)\sin(\beta x_2) \tag{30-14}$$

in which, ω is the natural frequency of the incompressible rectangular plate, and $i=(-1)^{1/2}$, U^{mn}, V^{mn}, W^{mn}, Θ_1^{mn}, Θ_2^{mn}, Θ_3^{mn}, Φ_1^{mn}, Φ_2^{mn}, Φ_3^{mn}, ψ_1^{mn}, ψ_2^{mn}, ψ_3^{mn}, P_0^{mn}, P_1^{mn} and P_2^{mn} are constant coefficients of the series solutions for the displacement field and the hydrostatic pressure components. Moreover, $\alpha=m\pi/a$ and $\beta=n\pi/b$, where m and n are the half wave numbers. Substituting equations (30) into the relations of the plate boundary conditions in Table 1, results in a homogeneous system of algebraic equations in terms of the mentioned constant coefficients. Finally, the determinant of the coefficient matrix is set equal to zero to find the natural frequencies.

6. Numerical Results and Discussion

In this section, natural frequencies are obtained for functionally gradated rectangular incompressible plates according to CPT, FSDT and TSDT. Also, to verify this research, the results are compared with those addressed in literature. In addition, to explore the effects of different material and geometrical parameters on vibrational behavior of those plates utilizing TSDT, mode shapes are plotted and studied in detail.

Consider a rectangular plate with length a, width b and uniform thickness h composed of an incompressible linear elastic functionally graded material as illustrated in Fig. 1. It is presumed that the functionally graded incompressible plate is composed of two types of rubber materials with the properties presented in Table 2.

Table 2 *Material properties of the constituents of the FG plate*

Incompressible material name	Young's Modulus	Density	Poisson's Ratio
Rubber 1	$E_1=4MPa$	$\rho_1=1300\,Kg/m^3$	$\nu=0.5$
Rubber 2	$E_2=0.7MPa$	$\rho_2=960\,Kg/m^3$	$\nu=0.5$

Natural frequencies of the plate are presented, here, in the following two non-dimensional forms

$$\hat{\omega}=\omega h\sqrt{\frac{\rho}{\mu}} \tag{31-1}$$

$$\overline{\omega}=\frac{\omega a^2}{h}\sqrt{\frac{\rho_1}{E_1}} \tag{31-2}$$

Table 3 *Comparison of non-dimensional natural frequencies $\hat{\omega}$ ×10 for incompressible thin homogeneous isotropic square plates (h/a=1/100, N=0)*

Mode (*m, n*)	Based on HSNDPT in Ref. [27]	Present study		
		TSDT	FSDT $(k_s = \pi^2/12)$	CPT
(1,1)	0.0114	0.0114	0.0080	0.0080
	0.4443	0.4443	0.4443	0.4443
(2,1)	0.0284	0.0284	0.0201	0.0201
	0.7025	0.7025	0.7025	0.7025
(1,0)	0.0057	0.0057	0.0040	0.0040
	0.3142	0.3142	0.3142	0.3142
(2,2)	0.0455	0.0455	0.0322	0.0322
	0.8888	0.8886	0.8886	0.8886
(3,1)	0.0568	0.0569	0.0402	0.0403
	0.9935	0.9935	0.9935	0.9935
(3,2)	0.0739	0.0739	0.0523	0.0524
	1.1327	1.1327	1.1327	1.1327
(2,0)	0.0228	0.0228	0.0161	0.0161
	0.6283	0.6283	0.6283	0.6283
(4,1)	0.0965	0.0965	0.0683	0.0684
	1.2953	1.2953	1.2953	1.2953
(3,3)	0.1022	0.1022	0.0724	0.0725
	1.3329	1.3329	1.3329	1.3329
(4,2)	0.1135	0.1135	0.0803	0.0805
	1.4050	1.4050	1.4050	1.4050

Table 3 presents the first two natural frequencies for thin incompressible functionally graded square plates for some mode numbers, *m* and *n*, and *N=0*. The first frequency refers to a bending mode and the second one refers to an in-plane mode. As shown in this table, both the in-plane and out-of-plane frequencies based on TSDT are in excellent accordance with those reported in reference [27] using HSNDT. Moreover, Table 3 indicates that the results of CPT and FSDT for thin plates are in good agreement with each other. This table also demonstrates that although the in-plane frequencies are the same for different plate theories, the bending frequencies obtained from CPT and FSDT are less than those obtained from HSNDT and TSDT considering the transverse shear and/or normal deformation effects. However, this difference cannot be due to the transverse shear and/or normal deformation effects because the thickness parameter (*h/a*) has been chosen to be very small and as a result there is no shear and normal deformation effect. In addition, ignoring the transverse shear and/or normal deformations by using CPT and/or FSDT should cause the plate stiffness and consequently the natural frequency to increase rather than decrease. As mentioned in the above sections, generally, based on CPT and FSDT the hydrostatic pressure *p* cannot participate in bearing any bending loads. This matter, however, stems from the fact that based on these theories, essentially the hydrostatic pressure *p* is considered to be invariable through the plate thickness direction and as a result it cannot generate any bending moment while according to HSNDT and TSDT, the hydrostatic pressure *p* contributes to bearing the bending loads due to its variable distribution along the plate thickness. Therefore, compared to HSNDT and TSDT, the bending stiffness of the incompressible plates according to CPT and FSDT is considered to be less, resulting in reduction of the bending natural frequencies. It means that for incompressible plates, the effect of the hydrostatic pressure *p* is more important than that of the shear and/or normal deformations.

Table 4 *Comparison of non-dimensional natural frequencies $\hat{\omega}$ for incompressible homogeneous square plates (h/a=1/20, N=0)*

Mode (*m, n*)	Ref.		Present study		
	[27] (HSNDPT)	[24] (3D Theory)	TSDT	FSDT $(k_s = \pi^2/12)$	CPT
(1,0)	-	-	0.0142	0.100	0.0101
(1,1)	0.0282	0.028	0.0282	0.0200	0.0201
(2,1)	0.0694	0.069	0.0693	0.0495	0.0501
(2,2)	0.1093	0.109	0.1093	0.0784	0.0799
(3,1)	0.1353	0.135	0.1353	0.0974	0.0997
(1,0)	0.1571	0.157	0.1571	0.1571	0.1571

(3,2)	0.1733	0.173	0.1733	0.1254	0.1292
(1,1)	0.2222	0.222	0.2221	0.2221	0.2221
(4,1)	0.2226	0.223	0.2226	0.1620	0.1683
(3,3)	0.2346	0.234	0.2346	0.1710	0.1780
(4,2)	0.2584	0.258	0.2584	0.1889	0.1974

Tables 4 and 5 compares the first twelve non-dimensional frequencies of a thin homogenous incompressible square plate by means of CPT, FSDT and TSDT with those reported in Refs. [24] and [27] using 3D elasticity theory and HSNDT, respectively. It can be obtained from these tables that the results of TSDT are in excellent agreement with those obtained from 3D elasticity theory and HSNDT. However, from these tables it can be concluded that although the results of CPT and FSDT are in a good accordance with each other, a significant difference is observed between their results with those of TSDT, HSNDT, and 3D elasticity theory. As mentioned earlier, this issue refers to the constant distribution of the hydrostatic pressure p along the plate thickness direction, considered by CPT and FSDT.

It can be interpreted from the results of Tables 3 to 5 that the classical and first-order shear deformation plate theories for homogenous incompressible plates are not as accurate as for the homogenous compressible ones, because their results for incompressible plates do not converge to the results of 3D and/or higher order theories even for very thin plates. Consequently, the higher order theories should be used whether the plate is either thin or thick.

Table 5 *Comparison of non-dimensional natural frequencies $\hat{\omega}$ for incompressible homogeneous square plates (h/a=1/12, N=0)*

Mode (m, n)	Ref.		Present study		
	[27] (HSNDPT)	[24] (3D Theory)	TSDT	FSDT $(k_s = \pi^2/12)$	CPT
(1,0)	-	-	0.0390	0.0277	0.0279
(1,1)	0.0768	0.077	0.0770	0.0549	0.0556
(2,0)	-	-	0.1499	0.1078	0.1107
(2,1)	0.1844	0.184	0.1851	0.1336	0.1379
(1,0)	0.2618	0.262	0.2618	0.2618	0.2618
(2,2)	0.2844	0.284	0.2860	0.2085	0.2189
(3,1)	0.3475	0.347	0.3498	0.2566	0.2721
(1,1)	0.3702	0.370	0.3702	0.3702	0.3702
(3,2)	0.4375	0.437	0.4411	0.3261	0.3510
(2,0)	0.5236	0.524	0.5236	0.5236	0.5236
(4,1)	0.5501	0.550	0.5556	0.4147	0.4541
(3,3)	0.5771	0.577	0.5831	0.4361	0.4796

Table 6 represents the first natural frequency of functionally graded incompressible plates for various thickness ratios and power law indices based on HSNDT, TSDT and FSDT. This table shows that for functionally graded incompressible plates similar to the homogenous ones, the results of FSDT are not in accordance with those of HSNDT and TSDT, justifying that the FSDT is not proper for vibrational analysis of incompressible plates even if the plate is moderately thick. This table, also, demonstrates that by increasing the plate thickness ratio, h/a, although the stiffness of the plate increases, $\bar{\omega}$ decreases. This issue, however, points to the fact that according to relation (31-2), the natural frequency is dimensionless respecting to the function h^2, and the growth of the denominator and the numerator respecting to h (or h/a) is not the same. Therefore, although the plate stiffness and consequently the natural frequency increases with increasing the thickness to length ratio, h/a, it is observed that the non-dimensional form of the frequency decreases. Therewith, it can be seen from this table that by increasing the power-law index N, $\bar{\omega}$ decreases because by increasing that parameter, volume fraction of the constitute with smaller Young's modules and consequently the plate stiffness decreases.

Table 6 *Effect of thickness ratio and power-law index on the non-dimensional natural frequencies for incompressible FG square plate using different plate theories*

$\frac{h}{a}$	$N=0$			$N=1$			$N=3$		
	HSNDT	TSDT	FSDT	HSNDT	TSDT	FSDT	HSNDT	TSDT	FSDT
1/2	3.8253	3.8264	3.2335	3.0523	3.0602	2.6583	2.5051	2.5049	2.3638
1/5	5.6831	5.6833	4.2648	4.3515	4.3617	3.5062	3.6901	3.7066	3.2006

1/10	6.3089	6.3090	4.5430	4.7687	4.7722	3.7349	4.1118	4.1188	3.4383
1/20	6.5082	6.5081	4.6242	4.8988	4.8996	3.8017	4.2496	4.2516	3.5090
1/50	6.5681	6.5681	4.6480	4.9384	4.9376	3.8212	4.2914	4.2918	3.5298

Table 7 *Effect of aspect ratio on the non-dimensional natural frequencies* $\bar{\omega}$ *for incompressible FG square plate using different plate theories*

$\frac{h}{a}$	$\frac{a}{b}=0.25$			$\frac{a}{b}=0.5$			$\frac{a}{b}=1$			$\frac{a}{b}=2$		
	HSNDT	TSDT	FSDT	HSNDT	TSDT	FSDT	HSNDT	TSDT	FSDT	HSNDT	TSDT	FSDT
1/2	2.4271	2.4275	1.9567	2.7395	2.7400	2.2348	3.8253	3.8264	3.2335	6.8894	6.8927	6.2386
1/5	3.2124	3.2124	2.3538	3.7298	3.7298	2.7472	5.6831	5.6833	4.2648	12.1931	12.1944	9.6384
1/10	3.4164	3.4164	2.4401	4.0036	4.0036	2.8643	6.3089	6.3090	4.5430	14.9191	14.9193	10.9890
1/20	3.4751	3.4751	2.4636	4.0842	4.0842	2.8967	6.5082	6.5081	4.6242	16.0144	16.0144	11.4573
1/50	3.4922	3.4922	2.4704	4.1078	4.1078	2.9061	6.5681	6.5681	4.6480	16.3769	16.3769	11.6029

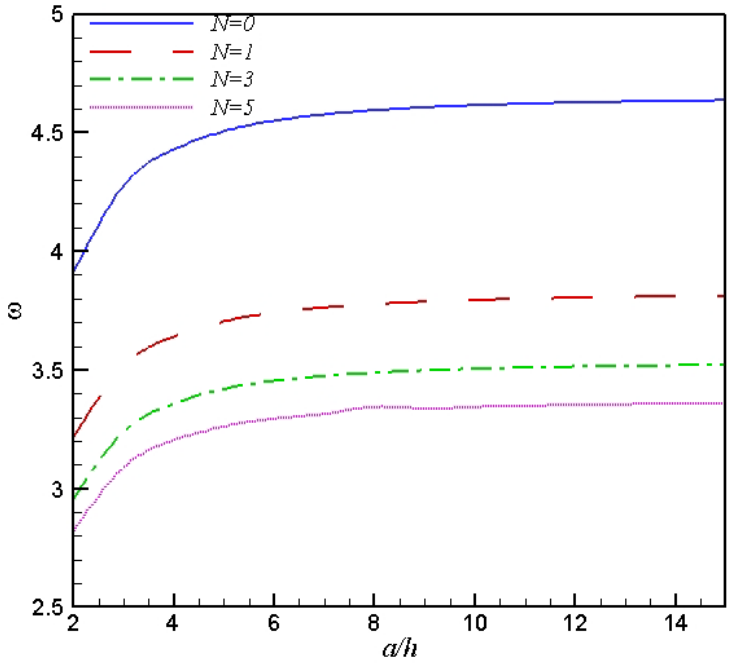

Fig. 2 *Non-dimensional frequency versus the thickness parameter for different values of power law index based on CPT*

Tables 7 studies the effect of the aspect ratio, *h/a*, on free vibration response of the FG incompressible plates for different plate theories. As this table shows, the natural frequency increases by increasing the aspect ratio, which is due to the decrease in the plate stiffness.

Fig. 2 plots the first non-dimensional frequency $\bar{\omega}$ versus the thickness parameter, *a/h*, for different power law indices, *N*, based on CPT. Similar results are presented in Figs. 3 and 4 based on FSDT and TSDT, respectively. It can be concluded from these figures that by increasing the thickness parameter, *a/h*, and/or by declining the power law index, *N*, the non-dimensional frequency increases. Furthermore, it is observed from these figures that as the power law index *N* reduces, the thickness parameter effect increases. Generally, with the reduction in the power-law index *N*, the material volume fracture with greater Young's modulus increases and as a result the stiffness of the plate rises. Also, by decreasing the length to thickness ratio, *a/h*, the stiffness of the plate increases. Therefore, it can be concluded that for smaller values of *N*, reducing the thickness parameter *a/h* increases the stiffness of the plate. Consequently, the thickness parameter effect, *a/h,* should is more significant for smaller power law indices, *N*. Moreover, these figures reveal that vibrational behavior of the FG incompressible plates is affected significantly by the magnitude of the parameter of power law index, *N*. Also, it can be observed that the effect of this parameter is increased by decreasing its value, which is due to the fact that for smaller values of *N*,

Int. Journal of Integrated Engineering Vol. 16 No. 1 (2024) p. 143-160

the volume fraction of the constitutes and consequently the FG plate material properties are more sensitive to that parameter.

Figs. 5 and 6 plot the normalized in-plane displacements mode shapes at the first bending vibrational mode along the thickness direction of the incompressible FG plate considering TSDT for various values of *N*. These figures show that, unlike the homogeneous plates, in-plane displacements for FG plates vary no longer linearly and symmetrically through the plate thickness. It is also observed from these figures that the top and bottom surfaces of the plate have, respectively, the most and the least in-plane deformation. This issue refers to the fact that Young' modulus of the material at the bottom surface is more than that at the top surface. Also, from these figures it can be obtained that upon increasing the power law index, *N*, the normalized in-plane deformations at the top surface decreases. It means that in the first vibrational mode, the more the power law index, the more difference between the in-plane deformations of top and bottom surfaces.

Fig. 7 illustrates the same plots for the plate deflection. This figure reveals that the plate deflection at the top and bottom surfaces is the same for homogenous plates (*N=0*). According to this figure, it is observed that the plate deflection has not a symmetric behavior with respect to the mid-plane for FG incompressible plates. In other words, a difference can be observed among the deflections of the top and bottom surfaces. Also, it visible that the deflection of the bottom surface is more than that of the top surface. As well, it is observed that by increasing the power law index, *N*, deflection of the top surface decreases. It means that by increasing the power law index, *N*, the plate thickness decreases in bending mode shapes.

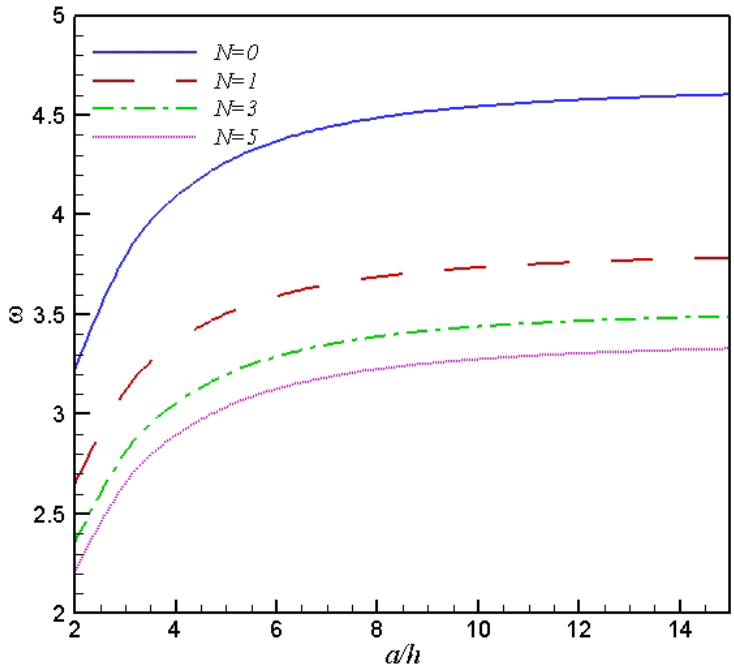

Fig. 3 *Non-dimensional frequency versus the thickness parameter for different values of power law index based on FSDT*

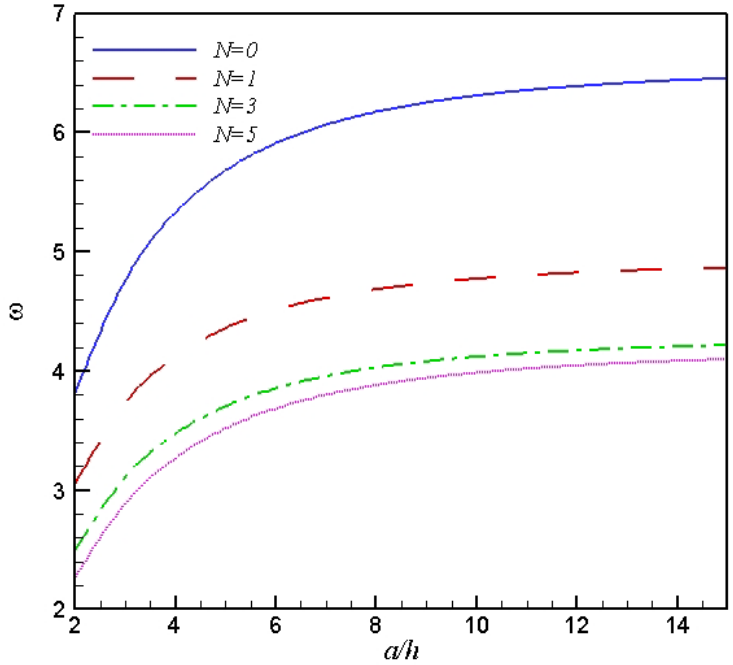

Fig. 4 *Non-dimensional frequency versus the thickness parameter for different values of power law index based on TSDT*

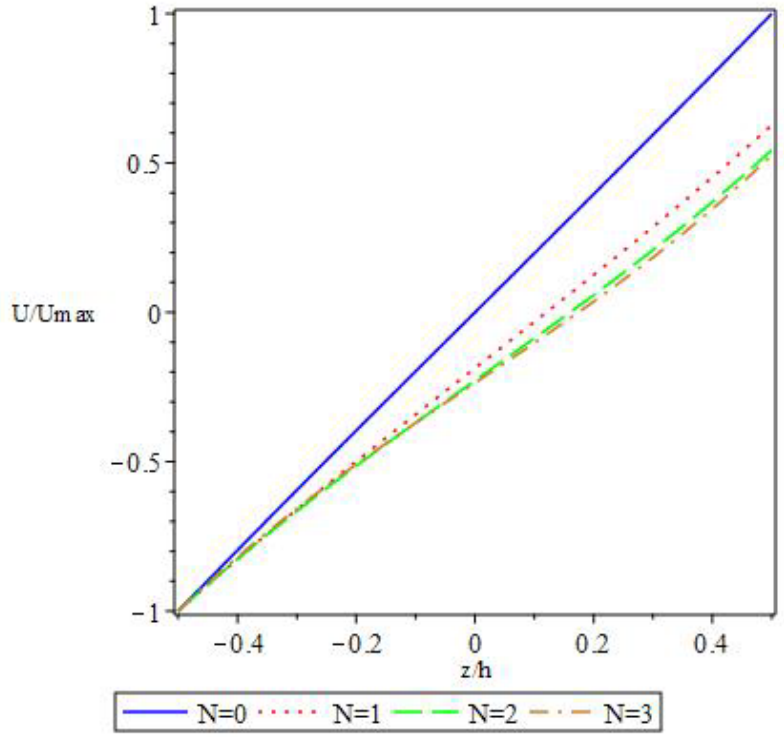

Fig. 5 *In-plane displacement mode shape of the incompressible FG plate versus the thickness direction using TSDT for various values of the power law index*

Int. Journal of Integrated Engineering Vol. 16 No. 1 (2024) p. 143-160

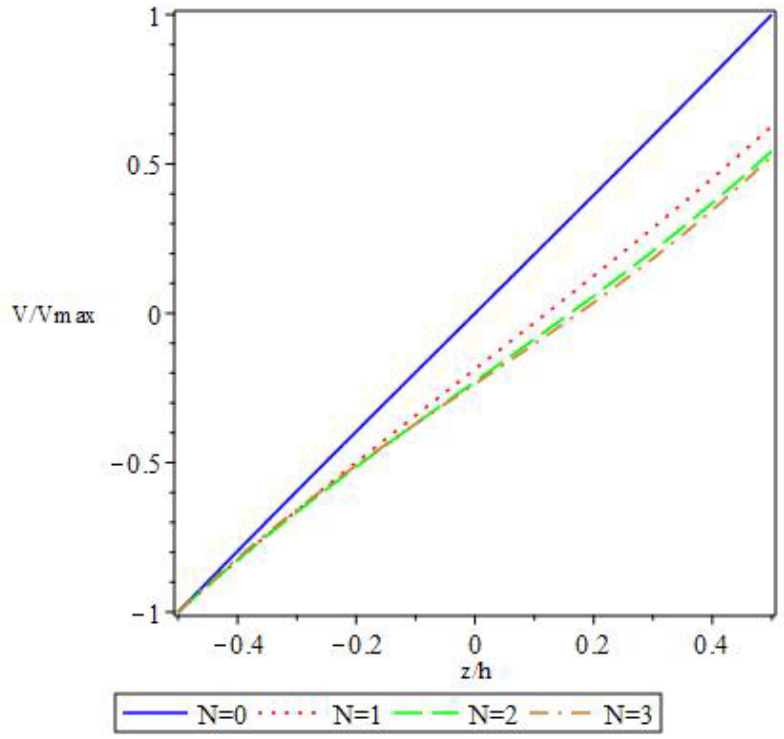

Fig. 6 *In-plane displacement mode shape of the incompressible FG plate versus the thickness direction using TSDT for various values of the power law index*

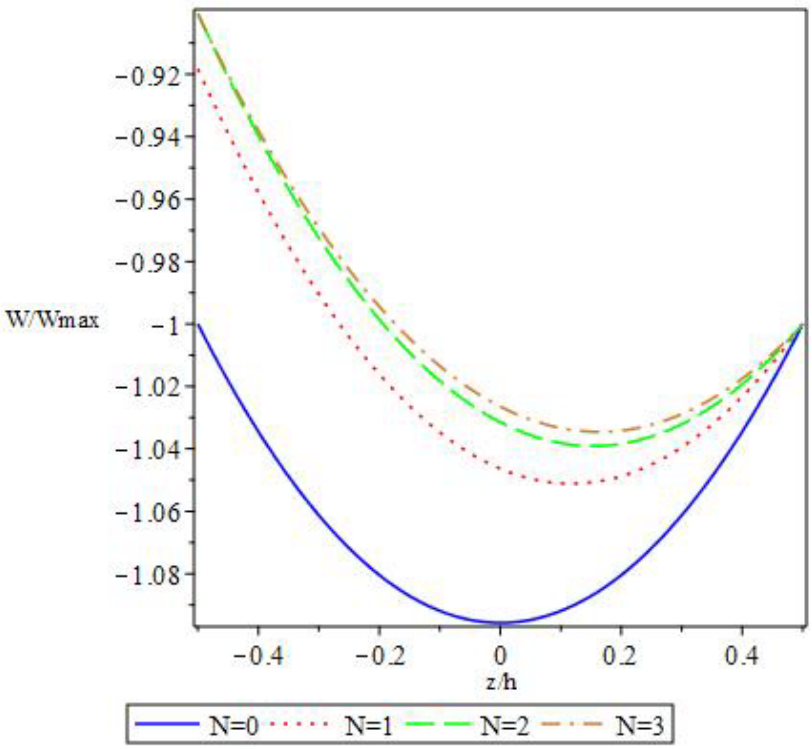

Fig. 7 *Deflection mode shape of the incompressible FG plate versus the thickness direction using TSDT for various values of the power law index*

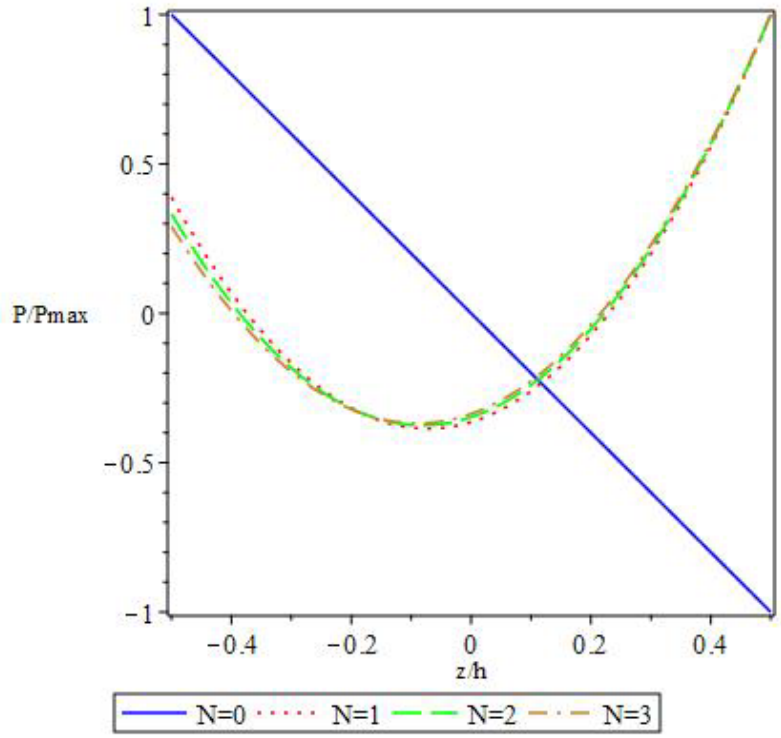

Fig. 8 *Hydrostatic pressure mode shape of the incompressible FG plate versus the thickness direction using TSDT for various values of the power law index*

The mode shape of the hydrostatic pressure, p, is depicted through the thickness in Fig. 8. This figure demonstrates that the hydrostatic pressure varies linearly through the plate thickness direction for homogeneous plates while it behaves completely nonlinear for the FG ones. This issue, however, refers to the nonlinear variation of the material properties of the FG plates along the thickness direction. It can be seen from this figure that unlike the homogeneous incompressible plates, the hydrostatic pressure at the top and bottom surfaces for FG plates has the same sign. Also, it is observed that the effect of the power law index, N, on vibrational mode shape of the hydrostatic pressure is not considerable.

7. Conclusion

This article studied free vibration analysis of incompressible functionally graded plates based on classical, first-order shear deformation, and third-order shear deformation plate theories. The plate material properties have been considered to vary through the plate thickness direction. The governing equations of motion together with the continuity equations have been solved analytically for rectangular simply supported plates to find the natural frequencies. Some comparisons have been done between results and those reported in the literature using HSNDT and 3D elasticity theory for homogenous incompressible plates. These comparisons have shown that the results of TSDT for both in-plane and out-of-plane vibration are in excellent accordance with those obtained from 3D elasticity theory and HSNDT, however, the results of CPT and FSDT for out of plane vibration of incompressible plates do not converge to the results of 3D elasticity theory, HSNDT and also TSDT, even for thin plates. It has been shown that this issue refers to the fact that unlike TSDT, HSNDT and 3D elasticity theory, according to CPT and FSDT, the hydrostatic pressure displays no role in bearing any bending load. Thus, CPT and FSDT consider the plate flexural stiffness to be less than the actual one, resulting in smaller values for the flexural frequencies. Therefore, it can be concluded that CPT and also FSDT for incompressible plates are not as precise as the compressible ones, and consequently, the higher order plate theories and/or three-dimensional elasticity theory are necessary for free bending vibrational analysis of incompressible plates, whether the plate is either thin or thick. Also, since TSDT is generally considered as a 2D theory, the solution procedure of this theory is less complicated than that of 3D theories such as HSNDT and 3D elasticity theory. Therefore, vibrational behavior of incompressible functionally graded plates has been studied in detail based on TSDT. The following results have been obtained:

i. The hydrostatic pressure effect is more significant than the shear and/or normal deformations effects.

ii. By increasing the power law index, the stiffness of the plate and consequently the natural frequencies decrease.
iii. The effect of the power law index on vibrational behavior of the FG incompressible plate is increased as its value decreases.
iv. As the plate thickness increases, the effect of the thickness parameter increases.
v. The thickness parameter effect increases by decreasing the power law index.
vi. Deflection, in-plane displacements, and the hydrostatic pressure is not symmetric with respect to the mid-plane for FG incompressible plates.
vii. In the first vibrational mode, the more the power law index, the more difference between the in-plane deformations of top and bottom surfaces of the plate.
viii. By increasing the power law index, the plate thickness decreases in bending mode shapes.
ix. The hydrostatic pressure varies nonlinearly through the plate thickness for FG incompressible plates.

Conflict of Interest

Authors declare that there is no conflict of interests regarding the publication of the paper.

Author Contribution

The authors confirm contribution to the paper as follows: ***study conception and design:*** A. Naderi*,* E. Mohseni*;* ***data collection:*** E. Mohseni, A. Naderi*;* ***analysis and interpretation of results:*** A. Naderi*;* ***draft manuscript preparation:*** A. Naderi*,* E. Mohseni, M. Mahmoudi Saleh Abaad*. All authors reviewed the results and approved the final version of the manuscript.*

References

[1] Cong, P.H., et al., *Nonlinear thermomechanical buckling and post-buckling response of porous FGM plates using Reddy's HSDT.* Aerospace Science and Technology, 2018. **77**: p. 419-428.
[2] Nwoji, C., et al., *Ritz variational method for bending of rectangular Kirchhoff plate under transverse hydrostatic load distribution.* Mathematical Modelling of Engineering Problems, 2018. **5**(1): p. 1-10.
[3] Naderi, A. and A. Saidi, *Buckling analysis of functionally graded annular sector plates resting on elastic foundations.* Proceedings of the Institution of Mechanical Engineers, Part C: Journal of Mechanical Engineering Science, 2011. **225**(2): p. 312-325.
[4] Demirhan, P.A. and V. Taskin, *Bending and free vibration analysis of Levy-type porous functionally graded plate using state space approach.* Composites Part B: Engineering, 2019. **160**: p. 661-676.
[5] Singh, S. and S.P. Harsha, *Buckling analysis of FGM plates under uniform, linear and non-linear in-plane loading.* Journal of Mechanical Science and Technology, 2019. **33**: p. 1761-1767.
[6] Abdollahi, M., A. Saidi, and M. Mohammadi, *Buckling analysis of thick functionally graded piezoelectric plates based on the higher-order shear and normal deformable theory.* Acta Mechanica, 2015. **226**(8): p. 2497-2510.
[7] Rouzegar, J. and F. Abad, *Free vibration analysis of FG plate with piezoelectric layers using four-variable refined plate theory.* Thin-Walled Structures, 2015. **89**: p. 76-83.
[8] Mojahedin, A., et al., *Buckling analysis of functionally graded circular plates made of saturated porous materials based on higher order shear deformation theory.* Thin-Walled Structures, 2016. **99**: p. 83-90.
[9] Ebrahimi, F. and S. Habibi, *Deflection and vibration analysis of higher-order shear deformable compositionally graded porous plate.* Steel and Composite Structures, 2016. **20**(1): p. 205-225.
[10] Chiker, Y., et al., *Free vibration analysis of hybrid laminated plates containing multilayer functionally graded carbon nanotube-reinforced composite plies using a layer-wise formulation.* Archive of Applied Mechanics, 2021. **91**: p. 463-485.
[11] Rezaei, A., et al., *Natural frequencies of functionally graded plates with porosities via a simple four variable plate theory: an analytical approach.* Thin-Walled Structures, 2017. **120**: p. 366-377.
[12] Cho, J.-R., *Hierarchic models for the free vibration analysis of functionally gradient plates.* International Journal of Mechanics and Materials in Design, 2021. **17**(3): p. 489-501.
[13] Hashemi, S., et al., *On the vibration of functionally graded annular plate with elastic edge supports and resting on Winkler foundation.* Australian Journal of Mechanical Engineering, 2023. **21**(3): p. 926-941.
[14] Ghatage, P.S. and P.E. Sudhagar, *Free Vibrational Behavior of Bi-Directional Functionally Graded Composite Panel with and Without Porosities Using 3D Finite Element Approximations.* International Journal of Integrated Engineering, 2023. **15**(1): p. 131-144.
[15] Ghatage, P.S., V.R. Kar, and P.E. Sudhagar, *On the numerical modelling and analysis of multi-directional functionally graded composite structures: A review.* Composite Structures, 2020. **236**: p. 111837.
[16] Chaudhary, S.K., V.R. Kar, and K.K. Shukla, *Flexural behavior of perforated functionally graded composite panels under complex loading conditions: higher-order finite-element approach.* Journal of Aerospace Engineering, 2021. **34**(6): p. 04021081.

[17] Ghatage, P.S. and P.E. Sudhagar, *Free vibrational behavior of bi-directional perfect and imperfect axially graded cylindrical shell panel under thermal environment.* Structural Engineering and Mechanics, 2023. **85**(1): p. 135.
[18] Kar, V.R., T.R. Mahapatra, and S.K. Panda, *Effect of different temperature load on thermal postbuckling behaviour of functionally graded shallow curved shell panels.* Composite Structures, 2017. **160**: p. 1236-1247.
[19] Joshi, K.K., et al., *Multi-Directional Graded Composites: An Introduction*, in *Advanced Composite Materials and Structures*. 2022, CRC Press. p. 1-11.
[20] Ghatage, P.S., et al., *Free Vibration Characteristics of Bi-Directional Functionally Graded Composite Panels*, in *Advanced Composite Materials and Structures*. 2022, CRC Press. p. 13-34.
[21] Gaspar, J., M. Loja, and J. Barbosa, *Static and free vibration analyses of functionally graded plane structures.* Journal of Composites Science, 2023. **7**(9): p. 377.
[22] Herrmann, L.R., *Elasticity equations for incompressible and nearly incompressible materials by a variational theorem.* AIAA journal, 1965. **3**(10): p. 1896-1900.
[23] Batra, R. and S. Aimmanee, *Vibration of an incompressible isotropic linear elastic rectangular plate with a higher-order shear and normal deformable theory.* Journal of sound and vibration, 2007. **307**(3-5): p. 961-971.
[24] Aimmanee, S. and R. Batra, *Analytical solution for vibration of an incompressible isotropic linear elastic rectangular plate, and frequencies missed in previous solutions.* Journal of sound and vibration, 2007. **302**(3): p. 613-620.
[25] Yuan, L. and R.C. Batra, *Vibrations of an incompressible linearly elastic plate using discontinuous finite element basis functions for pressure.* Journal of Vibration and Acoustics, 2019. **141**(5): p. 051016.
[26] Batra, R., *Higher-order shear and normal deformable theory for functionally graded incompressible linear elastic plates.* Thin-Walled Structures, 2007. **45**(12): p. 974-982.
[27] Mohammadi, M., E. Mohseni, and M. Moeinfar, *Bending, buckling and free vibration analysis of incompressible functionally graded plates using higher order shear and normal deformable plate theory.* Applied Mathematical Modelling, 2019. **69**: p. 47-62.
[28] Reddy, J.N., *Mechanics of laminated composite plates and shells: theory and analysis*. 2003: CRC press.
[29] Reddy, J.N., *Theory and analysis of elastic plates and shells*. 2006: CRC press.
[30] Mindlin, R., *Influence of rotatory inertia and shear on flexural motions of isotropic, elastic plates.* 1951.
[31] Mindlin, R.D., A. Schacknow, and H. Deresiewicz, *Flexural vibrations of rectangular plates.* 1956.
[32] Reissner, E., *On the theory of bending of elastic plates.* Journal of mathematics and physics, 1944. **23**(1-4): p. 184-191.
[33] Reddy, J. and J. Kim, *A nonlinear modified couple stress-based third-order theory of functionally graded plates.* Composite Structures, 2012. **94**(3): p. 1128-1143.
[34] Lai, W.M., D. Rubin, and E. Krempl, *Introduction to continuum mechanics*. 2009: Butterworth-Heinemann.
[35] Bao, G. and L. Wang, *Multiple cracking in functionally graded ceramic/metal coatings.* International Journal of Solids and Structures, 1995. **32**(19): p. 2853-2871.
[36] Reddy, J.N., *Energy principles and variational methods in applied mechanics*. 2017: John Wiley & Sons.